



CuO nanoparticles entrapped in MFI framework: Investigation of textural, magnetic and catalytic properties of Cu-ZSM-5 and Cu-S-1 catalysts

Giuseppe Fierro ^a, Giovanni Ferraris ^a, Giuliano Moretti ^{b,*}

^a Consiglio Nazionale delle Ricerche, Istituto dei Sistemi Complessi (ISC), Gruppo 'Materiali Inorganici e Catalisi Eterogenea' (MICE), c/o Dipartimento di Chimica, Università 'La Sapienza', P.le A. Moro 5, 00185 Roma, Italy

^b Dipartimento di Chimica, Università 'La Sapienza', P.le A. Moro 5, 00185 Roma, Italy

ARTICLE INFO

Article history:

Received 30 April 2009

Received in revised form 15 June 2009

Accepted 18 June 2009

Available online 24 June 2009

Keywords:

CuO nanoparticles

Cu-MFI catalysts

Textural properties

Magnetic susceptibility measurements

SCR of NO by propane

ABSTRACT

Cu-ZSM-5 zeolites are active catalysts for both NO decomposition and selective catalytic reduction (SCR) of NO by hydrocarbons in the presence of oxygen. Unfortunately they suffer of deactivation in the presence of water vapour in the feed that is mainly due to either the segregation of the initial extra-framework copper ions, or the sintering of the entrapped CuO-like species, to form large CuO aggregates on the external surface of the zeolite crystallites. In order to acquire more information about the nature of the CuO-like species which are formed upon dehydration of these materials at high temperature and the changes occurring to these species after catalysis, we investigated some Cu-ZSM-5 and Cu-S-1 catalysts by porosimetry and magnetic susceptibility measurements. Texture analysis revealed that, with respect to the H-ZSM-5 and S-1 parent materials, in the Cu-ZSM-5 and Cu-S-1 dehydrated samples a decrease of the surface area and micropore volume occurred, suggesting that most of the CuO-like species are entrapped into the zeolites channels. Consequently, their size has to fit the channel diameter (ca. 5.5 Å). This is confirmed by the magnetic results. Indeed, differently from bulk CuO, characterized by an antiferromagnetic behaviour, the magnetic susceptibility measurements of all the Cu-ZSM-5 samples followed the Curie–Weiss law typical of paramagnetic species. The lost of the antiferromagnetic behaviour supports the idea that the CuO-like particles are entrapped in the Cu-ZSM-5 channels as nanoclusters. On the other hand, the Cu-S-1 catalyst shows a complex magnetic behaviour, and peculiar textural modifications with respect to the S-1 parent material, suggesting that, with respect to those formed in Cu-ZSM-5, the CuO nanoclusters in this case are of a higher nuclearity and in a different location in the MFI structure. Under real catalytic conditions, i.e. in the presence of ca. 12% of water vapour in the feed, some changes occur to the CuO nanoparticles. In particular their structure seems to be affected. An increase in nuclearity is suggested that should lead to a decrease of the catalytic activity, as observed in the Cu-S-1 catalyst.

© 2009 Elsevier B.V. All rights reserved.

1. Introduction

Cu-ZSM-5 catalysts, which are active for important NO abatement reactions like the NO decomposition and the SCR of NO by hydrocarbons [1,2], are not stable enough to survive practical conditions, as for instance under high temperature in the presence of large amount of water vapour at the spark ignition engine exhaust gas [3]. The destruction of the active sites is caused by either the segregation of the initial extra-framework copper ions, or the sintering of the CuO-like species entrapped within the zeolite channels, to form large CuO aggregates on the external surface of the zeolite crystallites [3]. Much work has been done on

the characterization of the extra-framework copper ions, which are the active species for the NO decomposition [1,2], but more difficult is the study of the CuO-like species. They are probably the most active species for the SCR of NO by hydrocarbons in the presence of oxygen [1,3]. Entrapped CuO-like species are also formed by loading with copper ions the pure silicalite, S-1, that has the same MFI framework as the ZSM-5 zeolite but no Al³⁺ ions in the framework.

In spite of many efforts, the nature of the small CuO-like aggregates into the zeolites and its influence on the catalytic behaviour are not completely understood and are still the subject of an extensive debate [4]. Moved by that, we made a magnetic investigation of the copper species formed in Cu-ZSM-5 and Cu-S-1 zeolites upon dehydration at high temperature in air. The textural properties of these catalysts and of their parent H-ZSM-5 and S-1 materials were also investigated. The textural and the magnetic

* Corresponding author. Fax: +39 06 490324.

E-mail address: giuliano.moretti@uniroma1.it (G. Moretti).

susceptibility measurements provided complementary data on the nature and morphology of the CuO-like particles. Moreover, in order to check the influence of the catalytic conditions on these species, the magnetic analysis was also made on some catalysts after catalysis under real conditions for the SCR of NO at the spark ignition engine [3]. The nature of the copper species plays a fundamental role on the catalytic activity. In fact it is well known that the Cu-ZSM-5 samples are active catalysts for the SCR of NO by hydrocarbons and for the NO decomposition whereas, by contrast, the Cu-S-1 catalyst is almost inactive for both reactions [2,3]. It should be stressed that for the NO decomposition reaction only a few copper ions at peculiar extra-framework sites, related to the presence of aluminium, were suggested as active sites [2].

2. Experimental

2.1. Catalyst preparation

Details of the sample preparation have been reported elsewhere [2,3]. Briefly, the zeolite H-ZSM-5 and the homologous pure siliceous silicalite-1 (S-1) were prepared by using tetraethylsilicate, tetrapropylammonium hydroxide and a solution of Al^{3+} nitrate in ethanol, under hydrothermal treatment at 448 K for 24 h [2,3]. The crystalline product was separated from the liquid by centrifugation, then washed several times with water and dried for 2 h at 383 K. The dried powder was finally treated in air at a heating rate of 8.5 K/min from room temperature to 823 K, and then kept in air at 823 K for 5 h.

The cupric ions were exchanged into the H-ZSM-5 and the S-1 parent materials using copper acetate solutions at different concentrations in the range of 0.01–0.1 M. In particular, 2 g of zeolite was treated under stirring with 250 mL of a copper acetate solution at a desired concentration for 2 h at 323 K. The pH of the solution was constant at pH ≈ 5.5 regardless the copper ion concentration. Once the exchange step was completed, the solid was first washed with water, then dried in air at 383 K for 2 h (pale blue colour) and finally heated in air at 823 K for 5 h (green colour). The samples were stored at room temperature and at a relative humidity of 79% in a sealed vessel containing a saturated solution of NH_4Cl . Copper content was determined by atomic absorption (Varian SpectraAA-30). According to a standard nomenclature, the Cu-ZSM-5 catalysts are identified by the Si/Al ratio (kept constant in the present work at Si/Al = 80) and the percent of the nominal exchange value (e.g. Cu-ZSM-5-80-607). The nominal exchange value was calculated assuming that the full exchanged (100%) H-ZSM-5-80 parent material contains one Cu^{2+} ion for two framework Al^{3+} ions ($\equiv\text{Al}^{\text{---}}\text{O}^{\text{---}}\text{Si}\equiv$). On the other hand, since the S-1 parent material has no Al^{3+} ions and, therefore, no H^+ ions to be exchanged, the Cu-S-1 catalyst is identified only by the analytical copper content (Cu wt%).

2.2. Catalysts characterization

Textural analysis was performed by N_2 adsorption–desorption at 77 K using a Micromeritics ASAP 2010 analyzer. Before any measurement, all samples were preheated under vacuum along three temperature steps, namely at 423 K for 1 h, at 523 K for 1 h, and finally at 623 K for 4 h. The BET specific surface area, S_{BET} , was calculated using adsorption data in the relative pressure range $0 < P/P_0 < 0.1$. The mesopore size distribution was evaluated using the BJH method [5] from the adsorption data of the isotherm. The micropore volume, V_{μ} , (i.e. the empty volume contained in the MFI structure) and the external surface area, S_{ext} , (i.e. the specific surface area not contained in the micropore) were determined by t -test [6] in the t range from 5 to 15 Å for which the Harkins and Jura reference isotherm equation was used [7].

Magnetic susceptibility measurements were carried out in the range of temperature 90–300 K and at different magnetic field strengths of 4, 6, and 8 kG (1 G = 10^{-4} T) by using a Gouy balance. The instrument was first calibrated by using $\text{Co}[\text{Hg}(\text{CNS})_4]$. Samples were analyzed as prepared or after treatments (vide infra) in a sealed quartz tube. The magnetic susceptibility per mole, χ_m , ($\text{emu mol}^{-1} = \text{cm}^3 \text{mol}^{-1}$) was corrected for the diamagnetism of the quartz tube as well as for the H-ZSM-5-80 or S-1 parent materials. For the sake of comparison the magnetic susceptibility vs. temperature of a pure bulk CuO sample, prepared by thermal decomposition of $\text{Cu}_2(\text{OH})_2\text{CO}_3$ in air at 423 K for 6 h, was also measured.

2.3. Catalytic tests

Some of the catalysts investigated here have been previously tested under real lean conditions at the Istituto Motori of the Italian National Research Council (CNR), by using a spark ignition four cylinders engine (air/fuel mass ratio = 17). The exhaust gas composition was $\text{CO}_2 = 11\%$, $\text{H}_2\text{O} = 12\%$, $\text{O}_2 = 4\%$, $\text{NO}_x = 1240 \text{ ppm}$ [$\text{NO}/(\text{NO} + \text{NO}_2) = 0.9$], $\text{HC} = 420 \text{ ppm}$ (expressed as propane), $\text{CO} = 1310 \text{ ppm}$, $\text{N}_2 = \text{balance}$, space velocity of ca. $36,000 \text{ h}^{-1}$ [3].

Some results at 673 K are reported again in this work for the sake of comparison together with some data obtained in our laboratory for the SCR of NO by propane in the presence of oxygen. The catalytic tests were carried out in the steady state flow mode with the effluent gas analyzed by an on-line gas chromatograph. The typical reactant blend, i.e. $0.46\% \text{NO} + 0.46\% \text{C}_3\text{H}_8 + 5\% \text{O}_2 + \text{He}$ balance, was passed through the catalyst (100 mL (NTP)/min, 1 atm) at the space velocity of ca. $30,000 \text{ h}^{-1}$.

3. Results and discussion

3.1. MFI framework: composition and copper ion exchange capacity

Before reporting our data a brief analysis of the MFI structure may be helpful to the reader.

The unit cell (uc) of the H-ZSM-5 zeolite, MFI structure [8], may be theoretically written as



According to this formula the framework species are represented within square brackets while the extra-framework species are reported within vertical lines. Compared to the H-ZSM-5 material, which has Brønsted acid sites that can easily exchange protons with copper ions, in the S-1 zeotype no exchangeable protons may be theoretically present because there are no Al ions in the MFI framework (i.e. $a = 0$ in Eq. (1)). Therefore it was surprising when for the first time it was reported that S-1 has exchange properties [9].

It was found that if the MFI framework is synthesized by using tetraethylsilicate and tetrapropylammonium hydroxide as templating agent, a number of silicon vacancies may be present. In the zeotype S-1 these silicon vacancies cluster together forming silanols nests, as it has been demonstrated by means of high resolution neutron powder diffraction studies [10].

Woolery et al. first suggested that the internal silanols associated to the Si vacancies can be responsible of the Al-independent cation exchange capacity of S-1 [11].

There is now a general agreement that the internal silanol groups can have cation exchange capacity and we will use this concept writing the uc of S-1 as follows:

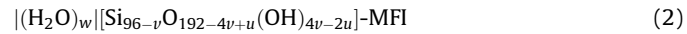


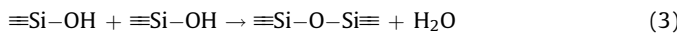
Table 1

Effect of MFI framework composition (Si/Al atomic ratio and Al ions per uc) and of the copper ion solutions pH on the copper loading of Cu-ZSM-5 and Cu-S-1 catalysts.

Sample	a/Al ions per uc	Cu wt% (% exchange) ^a (Cu acetate 0.1 M, pH ≈ 5.5)	Cu wt% (% exchange) ^a (Cu nitrate 0.1 M, pH ≈ 4.0)
Cu-ZSM-5-25-102	3.7	1.89 (102)	1.02 (55)
Cu-ZSM-5-40-324	2.3	3.79 (324)	–
Cu-ZSM-5-80-607	1.2	3.86 (607)	0.50 (84)
Cu-S-1	0.0	1.38	–

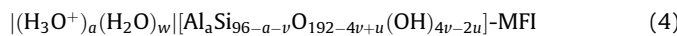
^a For all samples the ion-exchange step was done using 2 g of zeolite per 250 mL of solution under stirring for 2 h at 323 K [2,3,12,15].

where ' v ' represents the number of Si vacancies. The number of silanols produced by these defects is ' $4v$ ', and ' $2u$ ' represents the silanols that, in consequence of a high temperature treatment, lead to distorted Si–O–Si bridges according to the following reaction [10]:



As reported by Artioli et al. [10], the number of vacancies ' v ' ranges between 7 and 10 for a S-1 sample prepared using our procedure.

The uc of the H-ZSM-5, with nominal atomic ratio of Si/Al = $(96 - a)/a$, can be written as



The number of extra-framework water molecule per uc , ' w ', is influenced by the nature of extra-framework cations, by the ' a ', ' v ' and ' u ' values, by temperature and water vapour pressure at equilibrium in the gas phase.

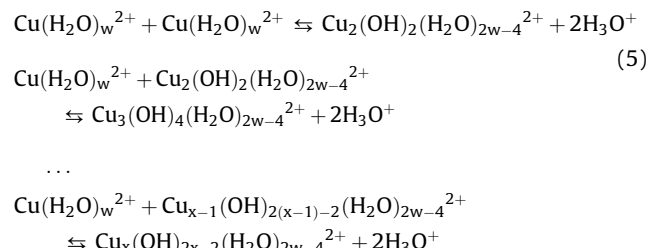
Previous literature data show that the number of defective sites per unit cell decreases as the number of aluminium ions increases [10,11].

The number of aluminium ions is not the only parameter influencing the exchanging properties, as suggested in Table 1 where the ion-exchange data for S-1 and some H-ZSM-5 parent materials are reported. The data in Table 1 suggest that the exchange properties depend on the Al content (i.e. the number of Brønsted acid sites $\equiv\text{Si}–\text{OH}–\text{Al}\equiv$), the number of internal silanols ($\equiv\text{Si}–\text{OH}$) and on the pH of the copper containing solutions. In the preparation of Cu-MFI samples reported in Table 1 the copper concentration is constant at 0.1 M and the different pH of the nitrate (pH ≈ 4.0) and acetate (pH ≈ 5.5) solutions is due to the hydrolysis of the acetate ion.

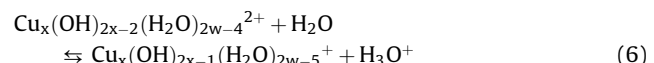
In Table 2, we report the copper loading and the relative % of exchange for the Cu-MFI catalysts investigated in this work. These catalysts were prepared using copper acetate solutions of different concentration (0.01–0.1 M) at constant pH ≈ 5.5. It appears that the ion-exchange with copper acetate solutions of the H-ZSM-5 ($a \approx 1.2$ Al ions per uc , Si/Al = 80) and S-1 ($a \approx 0$, Si/Al → ∞)

parent materials, leads easily to over-exchanged Cu-ZSM-5 and Cu-S-1 samples. In both cases the pH of the copper acetate solutions remains constant at pH ≈ 5.5 during the ion-exchange procedure. Therefore the over-exchange of copper ions cannot be ascribed to the precipitation of $\text{Cu}(\text{OH})_2$ within the zeolite channels [12]. In order to explain this phenomenon, the following equilibria in the copper ion solutions, as reported by Jolivet [13], may be invoked:

(i) condensation of copper cations by olation, which takes place by formation of hydroxo bridges



(ii) hydrolysis of the aquo-hydroxo complexes:



Although we do not know the equilibrium constant values of the above equilibria, from a qualitative point of view at high pH values they are shifted toward right. It has been reported that under this condition $\text{Cu}_x(\text{OH})_{2x-2}(\text{H}_2\text{O})_{2w-4}^{2+}$ is a linear polycation with edge bridges [13].

On the basis of the equilibria represented by Eqs. (5) and (6), the data reported in Table 1 suggest that $x \approx 1$ at low pH (copper nitrate solutions) with weak or no ion-exchange capacity of the internal silanols that are present in H-ZSM-5 zeolites with high Si/Al atomic ratio. On the other hand, at higher pH (copper acetate solutions), oligomeric copper hydroxo species ($x > 1$) may be present in solution. These species can be exchanged by the Brønsted acid sites (both $\equiv\text{Si}–\text{OH}–\text{Al}\equiv$ and internal silanols

Table 2

Results of the chemical and textural analysis (total surface area, S_{BET} , external surface area, S_{ext} and micropore volume, $V\mu$) for the Cu-ZSM-5-80 and Cu-S-1 catalysts and their H-ZSM-5-80 and S-1 parent materials.

Sample	$[\text{Cu}^{2+}]^a$ (M)	Cu wt%	c^b Cu per uc (% exchange)	$\Delta m_{\text{H}_2\text{O}}^c$ (%)	S_{BET} ($\text{m}^2 \text{g}^{-1}$)	S_{ext} ($\text{m}^2 \text{g}^{-1}$)	$V\mu$ (mL g^{-1})
H-ZSM-5-80	–	–	–	7.2	444	29	0.182
Cu-ZSM-5-80-207	0.01	1.35	1.24 (207)	8.0	409	39	0.163
Cu-ZSM-5-80-391	0.04	2.52	2.35 (391)	7.2	369	59	0.136
Cu-ZSM-5-80-498	0.08	3.19	2.99 (498)	5.5	393	30	0.159
Cu-ZSM-5-80-607	0.1	3.86	3.64 (607)	11	393	34	0.153
S-1	–	–	–	5.2	393	8	0.166
Cu-S-1	0.1	1.38	1.27	6.6	355	22	0.135

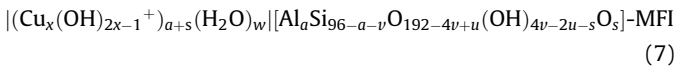
^a The ion-exchange step was done using 2 g of zeolite per 250 mL of copper acetate solution ($[\text{Cu}^{2+}] = 0.01/0.1 \text{ M}$) under stirring for 2 h at 323 K.

^b The chemical analysis was performed on samples heated in air at 823 K and then equilibrated at 79% relative humidity at room temperature. From Cu wt%, 'c' was calculated from the equation $c = (5767/63.55) \text{Cu wt\%}/(100 - \text{Cu wt\%})$. On the basis of Eq. (8) (see text), the uc molar mass was assumed $M_{uc} = (5767 + c63.55) \text{ g mol}^{-1}$. The Cu % exchange was calculated with the formula % exchange = $200c/(1.2)$.

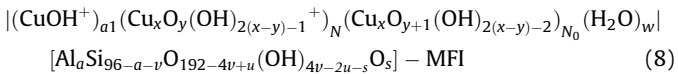
^c Total water loss% for samples heated in vacuum at 623 K. According to Eqs. (8) and (12), it should be calculated to a good approximation as following: $\Delta m_{\text{H}_2\text{O}}\% \approx 1802[w + (N_0 + N)(x - y - 1)]/(5767 + c63.55 + w18.02)$.

$\equiv\text{Si}-\text{OH}$) leading to over-exchanged Cu-ZSM-5 and Cu-S-1 samples. The data in Table 1 suggest that within the channels of H-ZSM-5 at low Si/Al ratio a local pH lower than that of the solution can be experienced, because the over-exchange phenomenon is suppressed ($x \rightarrow 1$).

According to Eq. (4), the as prepared Cu-MFI sample can be described by the following schematic formula:

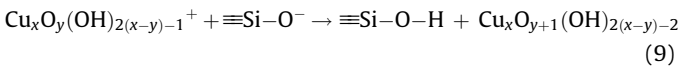


Upon a thermal treatment at high temperature and after conditioning at 79% relative humidity at room temperature, it is suggested that copper species turn mainly into copper oxo-hydroxo clusters that, on the basis of Eq. (7), can be schematically indicated as follows:



In this formula we assume an average nuclearity of the clusters, 'x', for either the positively charged and the neutral clusters, with $x \geq 2$ and $0 \leq y < x$. In particular, the copper species in Eq. (8) are

- (1) *isolated* copper species, such as CuOH^+ bonded to a fraction of $\equiv\text{Si}-\text{O}^-$ $\text{Al}\equiv$ sites. Two close CuOH^+ species could bring together forming the dimeric $\text{Cu}-\text{O}-\text{Cu}$ species already investigated [2]. They seem to be the active species for the NO decomposition over Cu-ZSM-5 catalysts. The number of such CuOH^+ ions per uc is a_1 ($a_1 < a$).
- (2) *positively charged* copper oxo-hydroxo clusters $\text{Cu}_x\text{O}_y(\text{OH})_{2(x-y)-1}^+$. The average number of such clusters per uc is N .
- (3) *neutral* copper oxo-hydroxo clusters $\text{Cu}_x\text{O}_{y+1}(\text{OH})_{2(x-y)-2}$. These species may be formed by interaction of $\text{Cu}_x\text{O}_y(\text{OH})_{2(x-y)-1}^+$ nanoclusters with the internal $\equiv\text{Si}-\text{O}^-$ sites, which are stronger bases with respect to $\equiv\text{Si}-\text{O}^-$ $\text{Al}\equiv$ sites:



The average number of such clusters per uc is N_0 .

According to Eq. (8), the balance of the number of copper ions per uc , 'c', obtained by chemical analysis, and the condition of electroneutrality of the uc lead, respectively, to the following equations:

$$c = a_1 + xN + xN_0 \quad (10)$$

$$a + s = N + a_1 \quad (11)$$

3.2. Porosimetry

The results of the characterization of the Cu-ZSM-5 (Si/Al = 80) and Cu-S-1 catalysts and their parent materials, H-ZSM-5 (Si/Al = 80) and S-1, are summarized in Table 2. In Fig. 1, the N_2 adsorption-desorption isotherms at 77 K of representative samples are reported. The data in Table 2 show that the textural features of the H-ZSM-5 parent material are affected by copper loading. Indeed the surface area and the micropore volume of all the Cu-ZSM-5 catalysts decreased with respect to the parent material. The same trend is observed for the S-1 and Cu-S-1 samples.

The decrease of the micropore volume suggests that the copper species in the over-exchanged Cu-ZSM-5 and Cu-S-1 catalysts are

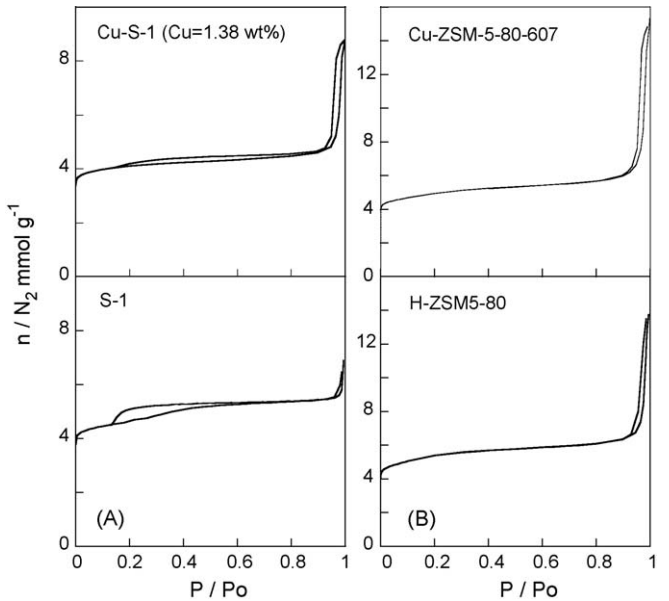
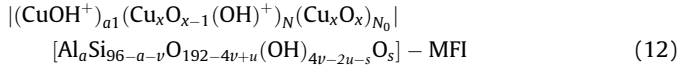


Fig. 1. N_2 adsorption-desorption isotherms at 77 K of (A) S-1 and Cu-S-1 ($\text{Cu} = 1.38$ wt%) and (B) H-ZSM5-80 and Cu-ZSM5-80-607.

entrapped in the MFI structure. Upon dehydration at high temperature in vacuum, the oxo-hydroxo nanoclusters tend to become oxidic nanoclusters. This process, on the basis of Eq. (8), can be schematically represented as follows:



These CuO nanoclusters may be located in the zeolite channels along the [1 0 0] and [0 1 0] directions (diameter ca. 5.5 Å), and/or in the cavities created at the channels intersection (diameter ca. 9 Å) [8]. They should be also located close to framework $\equiv\text{Si}-\text{O}^-$ $\text{Al}\equiv$ ions and in the supermicropores related to the presence of internal silanol nests and close to $\equiv\text{Si}-\text{O}^-$ ions and $\equiv\text{Si}-\text{OH}$ groups [14]. To support this view we could consider, to a first approximation, that the local structure of Cu_xO_x and $\text{Cu}_x\text{O}_{x-1}(\text{OH})^+$ nanoclusters resemble that of unit cell of CuO (monoclinic, 4 CuO formula per uc , $V_{uc} = 81.2 \text{ \AA}^3$, JCPDS file no. 5-0661,) or $\text{Cu}(\text{OH})_2$ (orthorhombic, 4 $\text{Cu}(\text{OH})_2$ formula per uc , $V_{uc} = 165 \text{ \AA}^3$, JCPDS file no. 35-505).

The decrease of micropore volume of the MFI framework with respect to the parent material can be roughly estimated by the following equation:

$$\Delta V\mu = (1/M)[x(N + N_0)(V_{uc}/4)N_A 10^{-24}] \quad (13)$$

where M is the molar mass (g/mol) of the zeolite uc ($M = 5767 + 63.55c$), N_A is the Avogadro number and, according to Eq. (10), $x(N + N_0) \approx c$. If the CuO , or $\text{Cu}(\text{OH})_2$, unit cell volume ($V_{uc} = 81.2 \text{ \AA}^3$ or $V_{uc} = 165 \text{ \AA}^3$) were inserted in Eq. (13), the $\Delta V\mu$ values would be in the range 0.01–0.02 mL g^{-1} in fairly good agreement with the experimental values (see Table 2).

In the case of S-1 and Cu-S-1 samples the textural analysis provided a more direct evidence to support the presence of CuO nanoclusters. In fact by comparing the isotherms of these samples, an important feature can be noticed (Fig. 1A). The isotherm of the S-1 parent material shows a hysteresis in the $0.15 < P/P_o < 0.4$ range which can be directly related to the filling up of micropores and narrow-mesopores [14]. This result is in agreement with the high resolution neutron powder diffraction studies of the zeotype S-1 that suggest a clustering of the Si vacancies to form silanols

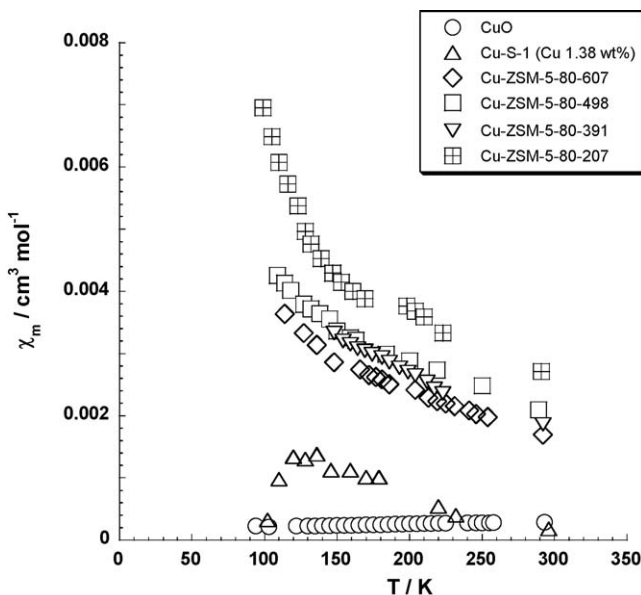


Fig. 2. Magnetic susceptibility measurements. χ_m vs. temperature plots for the as prepared (air 823 K 5 h) Cu-ZSM-5-80 and Cu-S-1 samples. For the sake of comparison, the data obtained for bulk CuO (mean crystallite size of 140 Å) are also shown.

nests [10]. Once copper is loaded in the S-1, the isotherm changes and shows a remarkable decrease of the hysteresis. This is also confirmed and reflected by a decrease ($\approx 0.03 \text{ mL g}^{-1}$) of the micropore volume (see Table 2). This finding clearly indicates that the cavities responsible in the S-1 matrix of the hysteresis in the $0.15 < P/P_0 < 0.4$ range are clogged by the CuO nanoparticles produced upon dehydration at high temperature of the Cu-S-1 sample [14]. Previous diffuse reflectance UV-vis spectra of Cu-ZSM-5-66-305 (Cu 2.24 wt%) and Cu-S-1 (Cu 1.38 wt%) samples [15] have shown that after a thermal treatment at 823 K in air for 4 h there are no evidence of absorption edges at $\approx 15320 \text{ cm}^{-1}$ ($\approx 1.9 \text{ eV}$) or at $\approx 11290 \text{ cm}^{-1}$ ($\approx 1.4 \text{ eV}$) due to the energy gap of large particles of Cu_2O and of CuO, respectively ($1 \text{ eV} = 96.48 \text{ kJ/mol} = 8065 \text{ cm}^{-1}$). However, it was reported [15] that the absorption due to d-d transitions of copper ions (d^9) in the Cu-S-1 sample extends at the higher wavenumbers with respect to the Cu-ZSM-5 sample, suggesting a possible higher nuclearity of the oxidic clusters in this materials. This d-d absorption band shifts from $\approx 12,000 \text{ cm}^{-1}$ to $\approx 13,500 \text{ cm}^{-1}$ while the shoulder at $\approx 14,000 \text{ cm}^{-1}$ shifts at $\approx 16,000 \text{ cm}^{-1}$. These effects can be attributed to an increased lateral interaction of copper ions in the Cu-S-1 sample which decreases the symmetry of the octahedral sites [15]. Moreover, in the Cu-S-1 sample there is also an absorption bands above $\approx 20,000 \text{ cm}^{-1}$ [15] that, according to Ismagilov et al. [4], may be assigned to ligand-metal charge-transfer band in larger clusters that extend along the zeolite channels.

3.3. Magnetic behaviour

The magnetic susceptibility of Cu-MFI samples provides the fingerprint of the magnetic interaction determined by multiple exchange couplings between pair of copper ions in CuO nanoclusters entrapped within the channels and cavities of the MFI framework. The origin of the net magnetic moments of antiferromagnetic CuO nanoparticles is still a matter of investigation due to the presence of complex phenomena related to uncompensated surface spins and size effects [16].

In Fig. 2, the magnetic susceptibility per mole of copper ion (χ_m) as a function of temperature in the range 90–300 K for the Cu-ZSM-

5-80 and Cu-S-1 samples is reported. Measurements were carried out on the as prepared samples, namely after a thermal treatment in air at 823 K for 5 h. In this figure the data obtained for a bulk CuO sample, prepared in our laboratory and characterized by particles with a mean crystallite size of 140 Å [17], have also been included for comparison.

From Fig. 2, it appears that Cu-ZSM-5-80, Cu-S-1 and bulk CuO show, each on its own, a peculiar and different magnetic behaviour. In particular, in the temperature range 90–300 K all the over-exchanged Cu-ZSM-5-80 samples follow the Curie–Weiss law typical of paramagnetic species [18]. By contrast, pure CuO is characterized by an antiferromagnetic behaviour, in agreement with literature data [19], and finally, the Cu-S-1 sample seems to behave in between.

The reciprocal of χ_m as function of temperature T for the Cu-ZSM-5-80 samples is fairly linear according to the Curie–Weiss law [18]:

$$\chi_m = \frac{C}{T - \theta} \quad (14)$$

The Curie constant, C , and the so-called Weiss temperature, θ , were obtained from χ_m^{-1} vs. T plots (not shown). From the Curie constant the effective magnetic moment, μ_{eff} , expressed in Bohr magneton (μ_B), can be calculated by the formula:

$$C = \left(\frac{\mu_{\text{eff}}}{2.83} \right)^2 \quad (15)$$

The μ_{eff} and θ values are reported in Table 3. The sign and absolute value of θ account, respectively, for the type and the strength of magnetic interactions among the paramagnetic species (ferromagnetic if $\theta > 0$ or antiferromagnetic if $\theta < 0$) [18].

In a previous characterization study we have found that a stoichiometrically exchanged Cu-ZSM-5-11-103 sample, obtained from ion-exchange of a Na-ZSM-5 (Si/Al = 11) zeolite with 0.01 M copper acetate solution at $\text{pH} = 6$, was characterized by a paramagnetic behaviour following the Curie–Weiss law [20]. After dehydration at 773 K, although most of the copper ions were present as isolated ions anchored to the zeolite framework in octahedral coordination through framework $\equiv \text{Si} - \text{O}^- - \text{Al} \equiv$ ions, a remarkable fraction (ca. 20%) segregated as CuO-like species [20].

In agreement with these previous results, and according to Eq. (12), in all our Cu-ZSM-5-80 and Cu-S-1 samples, besides isolated copper ions (CuOH^+), a significant fraction of CuO-like species, i.e. Cu_xO_x and $\text{Cu}_x\text{O}_{x-1}(\text{OH})^+$, may be present.

The magnetic results shown in Fig. 2 support the idea that the CuO-like species are entrapped within the channels and cavities of the MFI framework in the form of nanoparticles. They are loosing their antiferromagnetism, typical of a bulk CuO phase as well as of large CuO particles, and became superparamagnetic due to the increased amount of surface Cu^{2+} ions which are free to align with the magnetic field during the measuring time [21]. Indeed the existence of a superparamagnetic behaviour of CuO nanoparticles has been reported [16]. Accordingly, since the magnetic susceptibility of superparamagnetic particles decreases on increasing the particle size [21], the trend of magnetic susceptibility vs. temperature shown in Fig. 2 suggests that in Cu-ZSM-5-80 samples the size of the CuO nanoparticles increases on increasing the copper loading.

If we look at the Cu-S-1 sample, it has a copper content very close to that of the Cu-ZSM-5-80-207 catalyst but much less anchoring sites, this favouring the segregation of the copper species. Therefore it is expected that the number of segregated electroneutral Cu_xO_x nanoparticles per uc should be larger in Cu-S-1 than in the Cu-ZSM-5-80-207 preparation, and these species should also have higher ' x ' values. This is supported, as a whole, by the magnetic and textural data showing that the Cu-S-1 sample has

Table 3

Results of the magnetic measurements for Cu-ZSM-5-80 and Cu-S-1 catalysts.

Sample	Treatment	$\mu_{\text{eff}}/\mu_{\text{B}}^{\text{a}} (\pm 0.2)$	$\theta/K^{\text{b}} (\pm 10)$	H (kG)
Cu-ZSM-5-80-207	Air 823 K, 5 h	2.7	−48	8
Cu-ZSM-5-80-391	Air 823 K, 5 h	2.2	−31	8
		2.2	−24	6
Cu-ZSM-5-80-498	Air 823 K, 5 h	2.5	−82	8
Cu-ZSM-5-80-607	Air 823 K, 5 h	2.2	−57	8
		2.2	−53	6
		2.1	−55	4
Cu-ZSM-5-80-607	O_2 –3% H_2O , 823 K, 10 h	1.5	+30	8
Cu-ZSM-5-80-607	O_2 –3% H_2O , 823 K, 2.5 h	1.6	+14	8
	+ vacuum, 823 K, 0.5 h			
Cu-ZSM-5-80-607	After catalytic test under real conditions (20 h, 673 K in the presence of water)	4.7	−289	8
		5.0	−318	6
		5.7	−394	4
	Air 823 K, 5 h			
Cu-S-1 (Cu 1.38 wt%)		Antiferromagnetic-like 1.73		8
Cu^{2+} free ion		Antiferromagnetic		–
CuO^c				8
$Cu/\gamma-Al_2O_3^d$		1.91–2.00	0 to −20	–
$K_2Cu(SO_4)_2 \cdot 6H_2O^d$		1.91–1.97		–

^a μ_{eff} is the mean experimental magnetic moment (in Bohr magnetons) calculated from the Curie constant C obtained from the slope of χ^{-1} vs. T plots (see text). The theoretical spin-only magnetic moment of Cu^{2+} free ion ($S = 1/2$) is $\mu_{\text{eff}} = 2[S(S + 1)]^{1/2} \mu_{\text{B}} = 1.73 \mu_{\text{B}}$.

^b Weiss temperature, obtained as the intercept on the T axis of χ^{-1} vs. T plots (see text).

^c Mean crystallite size of ca. 140 Å (see Ref. [17]).

^d Data from Ref. [20].

the lowest magnetic susceptibility, it does not follow the Curie–Weiss law and is characterized by the largest decrease of the micropore volume and surface area with respect to the parent material (see Table 2). In the magnetic susceptibility vs. temperature curve of the Cu-S-1, a maximum is observed at ca. 130 K which may suggest the presence of ferro- and antiferromagnetic interactions with similar coupling constants [22].

The effective magnetic moment for all the as prepared Cu-ZSM-5-80 samples is slightly higher than $1.9 \mu_{\text{B}}$, which is the value expected for Cu^{2+} ions in octahedral coordination [20], and the θ values are always negative (see Table 3). The higher μ_{eff} values may reflect the formation of Cu_xO_x and $Cu_xO_{x-1}(OH)^+$ nanoparticles. The negative θ values and the independence of μ_{eff} from the magnetic field (see Table 3) may indicate that the interaction among Cu^{2+} ions via oxo and hydroxo bridges is mainly antiferromagnetic.

In Fig. 3, are shown the magnetic measurements vs. temperature for the Cu-ZSM-5-80-607 sample after the following treatments: (i) in air at 823 K for 5 h; (ii) in O_2 containing 3% H_2O for 10 h at 823 K; (iii) in O_2 containing 3% H_2O for 10 h at 823 K followed by outgassing in vacuum for 0.5 h at 823 K. The μ_{eff} and θ values measured after these treatments are reported in Table 3. Incidentally, the initial colour of the sample (green) does not change upon the treatment in O_2 containing water, but it turns into gray at the end of the treatment in vacuum. This is probably due to the change of symmetry around the Cu^{2+} ions caused by the loss of water molecules and the partial self-reduction of some Cu^{2+} ions to Cu^+ [2,3,12,20].

The Cu-ZSM-5-80-607 sample treated at high temperature with O_2 containing 3% of water vapour in the feed, no matter the final treatment in vacuum, presents effective magnetic moments slightly lower than $1.9 \mu_{\text{B}}$ and values of the Weiss temperature slightly positive. The latter finding indicates that the interaction among the Cu^{2+} ions becomes mainly ferromagnetic. It was found that CuO nanoparticles can exhibit also a ferromagnetic character [16].

In Fig. 4, the magnetic measurements vs. temperature, and at different magnetic field strength, for the over-exchanged Cu-ZSM-5-80-607 catalyst as prepared and after the catalytic tests under real conditions (20 h at 673 K in the presence of water) [3] are shown. As reported in Table 3 after the catalytic test the effective magnetic moment increases and the Weiss temperature become largely negative, suggesting the aggregation of Cu_xO_x and $Cu_xO_{x-1}(OH)^+$ in nanoparticles of higher nuclearity, a process

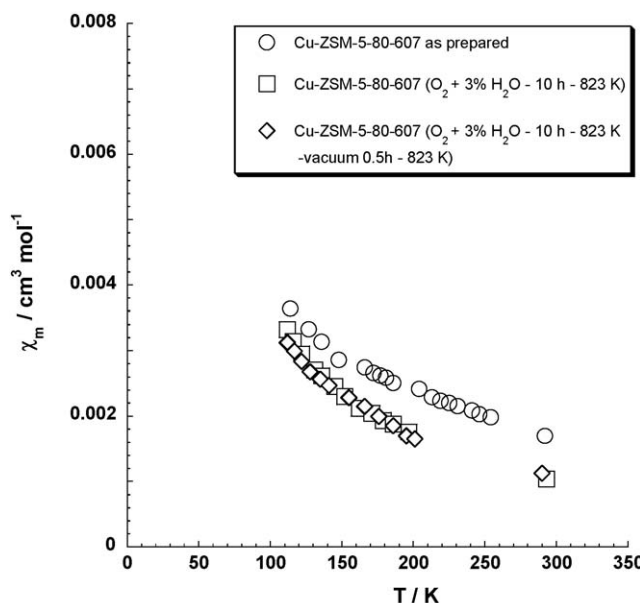


Fig. 3. Magnetic susceptibility measurements. χ_m vs. temperature plots for the Cu-ZSM-5-80-607 catalyst as prepared (air 823 K 5 h) and after treatments under the following conditions: (i) in O_2 containing 3% H_2O for 10 h at 823 K, (ii) in O_2 containing 3% H_2O for 10 h at 823 K followed by outgassing in vacuum for 0.5 h at 823 K.

Table 4

Catalytic activity of Cu-ZSM-5-80 and Cu-S-1 catalysts at 673 K for the HC-SCR of NO.

Catalyst	Cu wt%	NO conversion (%)	Note
S-1	–	≈0	Absence of H ₂ O in the feed The S-1 parent material is not active while the H-ZSM-5 parent material present a conversion comparable to that of the Cu-S-1 catalyst. Cu-ZSM-5-80 catalysts are highly active. The activity of all the catalysts is stable in the absence of H ₂ O in the feed.
Cu-S-1	1.38	11	
H-ZSM-5-80	–	14	
Cu-ZSM-5-80-391	2.52	≈100	
S-1	–	≈0	Presence of ca. 12% H ₂ O in the feed (Ref. [3]) In the real lean-burn gasoline engines the H-ZSM-5 and S-1 parent materials and Cu-S-1 sample are not active.
Cu-S-1	1.38	≈0	The NO _x conversion for all Cu-ZSM-5-80 catalysts tends to decrease with time on stream and after 30–40 h becomes negligible. The values here reported are the initial conversions at 673 K.
H-ZSM-5-80	–	≈0	The rate of deactivation is higher for the catalysts with the lowest Cu loading: after 20 h on stream the NO _x conversion for Cu-ZSM-5-80-207 is only 5%, while the conversion of Cu-ZSM-5-80-607 is about 20%.
Cu-ZSM-5-80-207	1.35	39	
Cu-ZSM-5-80-391	2.52	37	
Cu-ZSM-5-80-607	3.86	37	

facilitated by the high temperature and the presence of water vapour [3]. Moreover the magnetic susceptibility becomes dependent on the magnetic field suggesting the formation of ferromagnetic domains as the size of the CuO nanoparticles increases.

3.4. Catalytic tests

The catalytic results are reported in Table 4. The results of the SCR with propane of NO in the presence of O₂ at 673 K (no water vapour in the feed) show that the S-1 parent material is not active at all. By contrast, the Cu-S-1 and H-ZSM-5-80 samples show a similar, rather low, activity. A complete NO conversion occurs over Cu-ZSM-5-80-391 catalyst. As regards the selectivity to N₂, S_{N2}, only the H-ZSM-5-80 sample shows a little amount of N₂O among

the products (S_{N2} = 0.96). For all the copper-containing catalysts, S_{N2} reaches 100% at 673 K. Moreover, the catalytic activity is not influenced by the time of stream in the reactant mixture (experimentally up to 10 h on stream).

Under real lean-burn gasoline engines conditions (presence of ca. 12% of water vapour in the reactant mixture), as previously found [3], the H-ZSM-5-80, S-1 and Cu-S-1 samples are not active at all while the activity of Cu-ZSM-5-80 catalysts is independent of copper loading. The catalysts, however, are not stable on prolonged time on stream [3]. Under these conditions it seems that higher copper loadings tend to stabilize the activity of Cu-ZSM-5-80 catalysts for a limited time on stream, an effect probably related to the high mobility of smaller clusters at high temperature in the presence of water. The major role played by water vapour in the deactivation process was clearly demonstrated by removing water from the exhaust gas. Under this condition, the conversions of the pollutants remained constant up to 20 h on stream [3]. The nuclearity of Cu_xO_x and Cu_xO_{x-1}(OH)⁺ oxo-hydroxo nanoclusters increases in the presence of water leading to a loss of catalytic activity that eventually completely disappears as large CuO particles are formed at the external surface of the zeolite. In fact, the X-ray diffraction analysis of the catalyst at the end of the catalytic runs (30–40 h on stream) revealed the presence of the CuO pattern, suggesting that CuO particles larger than ca. 50 Å segregated at the external surface of the zeolite crystallites [3].

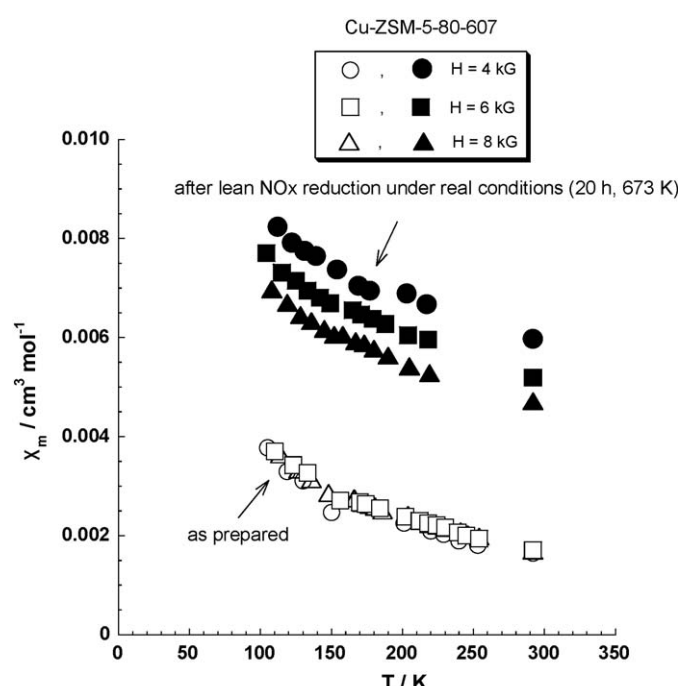
4. Conclusions

The results reported in this work suggest that in over-exchanged Cu-ZSM-5-80 catalysts CuO nanoparticles may be entrapped within the MFI framework and behave as paramagnetic species, contrary to the antiferromagnetic behaviour of bulk CuO. On the other hand, the CuO nanoparticles entrapped in Cu-S-1 are characterized by a complex magnetic behaviour, suggesting that their size and structure are different from the CuO nanoparticles in Cu-ZSM-5-80. The size of the CuO nanoparticles markedly affects the catalytic behaviour. In fact, the catalytic tests showed that the Cu-ZSM-5-80 samples are active catalysts for both the SCR by propane in presence of excess O₂ and for the NO_x reduction under real lean-burn gasoline engines conditions. On the contrary Cu-S-1 is practically inactive for both the reactions.

Acknowledgment

We thank Dr. Dino Fiorani for fruitful discussions about the magnetic susceptibility measurements.

Fig. 4. Magnetic susceptibility measurements. χ_m vs. temperature plots at different magnetic field strengths for the Cu-ZSM-5-80-607 catalyst as prepared (air 823 K 5 h) and after lean NO_x-SCR under real conditions (20 h at 673 K in the presence of water).



Appendix A. Supplementary data

Supplementary data associated with this article can be found, in the online version, at doi:10.1016/j.apcatb.2009.06.020.

References

- [1] M. Shelef, Chem. Rev. 95 (1995) 209–225.
- [2] G. Moretti, G. Ferraris, G. Fierro, M. Lo Jacono, S. Morpurgo, M. Faticanti, J. Catal. 232 (2005) 476–487.
- [3] G. Moretti, G. Minelli, P. Porta, P. Ciambelli, P. Corbo, M. Gambino, F. Migliardini, S. Iacoponi, Stud. Surf. Sci. Catal. 105 (1997) 1525–1532; P. Ciambelli, P. Corbo, M. Gambino, G. Minelli, G. Moretti, P. Porta, Catal. Today 26 (1995) 33–39.
- [4] Z.R. Ismagilov, S.A. Yashnik, V.F. Anufrienko, T.V. Larina, N.T. Vasenin, N.N. Bulgakov, S.V. Vosel, L.T. Tsykoza, Appl. Surf. Sci. 226 (2004) 88–93.
- [5] E.P. Barrett, L.G. Joyner, P.H. Halenda, J. Am. Chem. Soc. 73 (1951) 373–380.
- [6] S.J. Gregg, K.S.W. Sing, Adsorption, Surface Area and Porosity, Academic Press, London, 1982, p. 94.
- [7] W.D. Harkins, G. Jura, J. Am. Chem. Soc. 66 (1944) 1362–1366.
- [8] Ch. Baerlocher, W.M. Meier, D.H. Olson, Atlas of Zeolite Framework Types, Fifth Revised Edition, Elsevier, 2001, pp. 184–185.
- [9] A.W. Chester, Y.F. Chu, R.M. Dessa, G.T. Kerr, C.T. Kresge, J. Chem. Soc., Chem. Commun. (1985) 289–290.
- [10] G. Artioli, C. Lamberti, G.L. Marra, Acta Crystallogr. B 56 (2000) 2–10.
- [11] G.L. Woolery, L.B. Alemany, R.M. Dessa, A.W. Chester, Zeolites 6 (1986) 14–16.
- [12] G. Moretti, G. Ferraris, P. Galli, Stud. Surf. Sci. Catal. 135 (2001) 5020–5028.
- [13] J.-P. Jolivet, Metal Oxide Chemistry and Synthesis, J. Wiley & Sons, Ltd., Chichester, 2000, pp. 78–80.
- [14] G. Moretti, G. Ferraris, G. Fierro, Stud. Surf. Sci. Catal. 174 (2008) 925–928.
- [15] C. Dossi, A. Fusi, S. Recchia, R. Psaro, G. Moretti, Micropor. Mesopor. Mater. 30 (1999) 165–175.
- [16] G. Narsinga Rao, Y.D. Yao, J.W. Chen, IEEE Trans. Magn. 41 (2005) 3409–3411.
- [17] G. Moretti, G. Fierro, M. Lo Jacono, P. Porta, Surf. Interface Anal. 14 (1989) 325–336.
- [18] C.J. O'Connor, Prog. Inorg. Chem. 29 (1982) 203.
- [19] M. O'Keeffe, F.S. Stone, J. Phys. Chem. Solids 23 (1962) 261–266.
- [20] M. Lo Jacono, G. Fierro, R. Dragone, X. Feng, J. d'Itri, W.K. Hall, J. Phys. Chem. B 101 (1997) 1979–1984.
- [21] J.L. Dormann, D. Fiorani, E. Tronc, Adv. Chem. Phys. 98 (1997) 283.
- [22] G. De Munno, M. Julve, F. Lloret, J. Faus, M. Verdaguer, A. Caneschi, Inorg. Chem. 34 (1995) 157–165; M. Lubben, R. Hage, A. Meetsma, K. Byma, B.L. Feringa, Inorg. Chem. 34 (1995) 2217–2224.